Study on the Foaming of Crosslinked Polyethylene

SHIGEHIKO ABE, MASAYUKI YAMAGUCHI

Yokkaichi Research Laboratory, TOSOH Corporation, 1-8 Kasumi, Yokkaichi, Mie, 510-8540 Japan

Received 19 January 2000; accepted 7 June 2000

ABSTRACT: The processing of crosslinked polyethylene foam, which has a closed-cell structure, has been investigated. In this study, two types of linear low-density polyethylene (LL) produced by a metallocene catalyst were crosslinked by dicumyl peroxide (DCP). The expansion ratio of the foams decreases with increasing the DCP content, which is due to the enhancement of the elastic modulus. Moreover, the crystallization temperature T_c of the foams is also responsible for the expansion ratio. After expansion, the crosslinked foam with lower T_c shrinks to a great degree prior to the crystallization, which is attributed to the volume reduction of the gas in the cells. As a result, the expansion ratio decreases. The degree of shrinkage decreases with increasing the T_c, because immediate crystallization prevents the shrinkage. © 2001 John Wiley & Sons, Inc. J Appl Polym Sci 79: 2146–2155, 2001

Key words: linear low-density polyethylene; crosslinked polyethylene; rheological property; foam processing; crystallization

INTRODUCTION

Crosslinked polyethylene (XL-PE) foams have various kinds of applications, such as thermal insulation, floatation, automotive trim, and sports goods. Up to now, high-pressure low-density polyethylene (LD) has been mainly used for the production of XL-PE foams.[1–3] Recently, however, much attention has been focused on the linear low-density polyethylene (LL) produced by a metallocene catalyst as a substitute for the conventional LD. This is plausible because the LL produced by a metallocene catalyst exhibits lower modulus and excellent mechanical properties.[4–10] Therefore, it is of considerable importance for the industrial application to comprehend the effect of the molecular architecture such as short chain branching on the cellular structure. In particular, the prediction of the expansion ratio, which governs the mechanical properties of the foam, is very important for the decision of the recipe for the XL-LL foam.

In this article, the foam processing of the XL-LLs was studied. We investigated the rheological properties of the XL-LLs first, because they would be important for the foaming behavior. Then the relation between rheological properties and expansion ratio has been discussed. Moreover, two types of the LL with different number of short chain branches, which were produced by a metallocene catalyst, were employed for the better understanding of the effect of the molecular structure on the foaming.

EXPERIMENTAL

Polymers and Sample Preparation

Two types of ethylene-1-hexene copolymers, LL1 and LL2, produced by a metallocene catalyst were used in this study. The contents of 1-hexene in the copolymers were determined from ^{13}C nuclear magnetic resonance spectroscopy; the LL1 has 25

Correspondence to: Shigehiko Abe (s_abe@tosoh. co.jp).

Journal of Applied Polymer Science, Vol. 79, 2146–2155 (2001)

branches and the LL2 has 7 branches per 1000 backbone carbon atoms. The number, weight, and *z*-average molecular weights, which were determined by gel permeation chromatography (Waters, 150-C) in *ortho*-dichlorobenzene at 408 K, were $M_n = 4.6 \times 10^4$, $M_w = 8.3 \times 10^4$, $M_z = 1.4 \times 10^5$ for the LL1, and $M_n = 4.6 \times 10^4$, $M_w = 9.0 \times 10^4$, $M_z = 1.5 \times 10^5$ for the LL2, as a polyethylene standard.

The foams were obtained by one-shot press-molding method. The preformed compounds were composed of 100 parts of a polymer containing 0.1–0.9 wt % of dicumylperoxide (DCP) as a crosslinking agent and 8 phr of a blowing agent. The compounds were blended using a two-roll mill in which the surface temperature was kept at 423 K. The blowing agent is a mixture of 50% of dinitrosopentamethylenetetramine and 50% of urea. The molding condition was as follows: temperature is 438 K, pressure is 20 MPa, and duration time is 20 min. Under this condition, the blowing agent fully decomposed. After removal of the pressure, expansion takes place immediately. Then the obtained foam was left at room temperature until it was cooled down. For the sake of the investigation on the rheological properties, crosslinked polyethylenes were also prepared without the blowing agent. The method was the same as that for the preparation of the foam.

The following nomenclature is used throughout. LL1 and LL2 are originally polyethylenes, which contain neither peroxide nor blowing agent. XL-LL(x) is the crosslinked LL with x wt % of DCP. XL-LL(x) foam is the foam with x wt % of DCP and 8 phr of the blowing agent.

Measurements

Thermal properties were measured using a differential scanning calorimeter (Perkin-Elmer, DSC-7) under nitrogen atmosphere . An indium standard was to calibrate the temperature and enthalpy of fusion. The samples of about 10 mg weight sealed in aluminum pans were heated from room temperature to 463 K at a heating rate of 10 K min^{-1}. After holding 5 min at 463 K, the samples were cooled down to room temperature at a cooling rate of 10 K min^{-1}.

Gel fraction and degree of swelling were measured by a solvent extraction technique following the method developed by de Boer and Penning.[11] The gel fraction ϕ_g was determined by the ratio of the weight of dried extracted w_g to initial weight w_i as

$$\phi_g = \frac{w_g}{w_i} \tag{1}$$

The degree of swelling q was calculated by the ratio of the weight of swollen gel w, to the weight of dried extracted w_g as

$$q = \frac{w_s}{w_g} \tag{2}$$

Oscillatory shear moduli, such as shear storage modulus G' and loss modulus G'', of the LLs were measured using a cone-plate type rheometer (Rheology, MR-500) at temperatures between 433 and 493 K. The time–temperature superposition was applied to frequency dependence of oscillatory shear moduli at different temperatures in an attempt to determine the linear viscoelastic properties over a wide range of time scale. All measurements were carried out under nitrogen atmosphere in order to avoid thermooxidative degradation. Those of the XL-LLs were measured at 438 K using a parallel-plate geometry in the angular frequency range of 1.00×10^{-2} to 3.14×10^{1} s^{-1}.

Stress–strain curves were measured using a dynamic mechanical analyzer (Rheology, DVE V-4), which was improved to have the capability of subjecting a specimen to elongate at a constant stretching rate. The following conditions were employed: temperature is 438 K, the initial length between the clumps is 20 mm, and the elongational rate is 1.0 mm min^{-1} (strain rate is 8.33×10^{1} s^{-1}). The stress was determined from dividing the tensile load by the initial cross-sectional area, and the strain was calculated from the ratio of the increment of the length between clamps to initial length.

Expansion ratio E_R of the foams is given by the following relation:

$$E_R = \frac{\rho_p}{\rho_f} \tag{3}$$

where ρ_p is the density of the prefoamed material and ρ_f is that of the foam at 293 K, which were measured by a buoyancy method using a densimeter (Toyoseiki, Archimedes).

RESULTS AND DISCUSSION

Polymer Characteristics

As well known, short chain branching much affects the thermal and mechanical properties of

LL.[4–10,12,13] In particular, melting point T_m, crystallization temperature T_c, and heat of fusion decrease rapidly with increasing the number of short chain branches. Moreover, depression of T_m for the LL produced by a metallocene catalyst is more prominent than that for the conventional LL produced by a Zieglar–Natta catalyst, which is owing to the homogeneous incorporation of short chain branches into the polymer chain. The values obtained from the DSC heating run in this study, T_m = 369.8 K for the LL1 and T_m = 390.2 K for the LL2 agree well with the literature.[14]

Figure 1 shows master curves of frequency dependence of oscillatory shear moduli for the LL1 [Fig. 1(a)] and the LL2 [Fig. 1(b)]. The reference temperature is 463 K. Over the range of interest, the results of both LLs were found to obey the principle of the time–temperature superposition. Therefore, the apparent activation energy ΔH_a can be calculated from the temperature dependence of shift factor a_T using the Arrhenius equation. Consequently, the ΔH_a is found to be 35.0 kJ mol^{-1} for the LL1 and 28.0 kJ mol^{-1} for the LL2. According to Vega et al.,[15] ΔH_a for the LL is determined by the number of short chain branches as

$$\Delta H_a = 23.9 + 26.8\left[1 - \exp\left(-\frac{n}{35.4}\right)\right] \quad (4)$$

where n is the number of short chain branches per 1000 backbone carbon atoms. Following the equation, the ΔH_a is calculated to be 37.4 kJ mol^{-1} for the LL1 and 28.4 kJ mol^{-1} for the LL2. The latter corresponds to our experimental value within experimental error, although the former is smaller than predicted value. From the results, eq. (4) seems to be valid when n is below 25. Furthermore, it is found from Figure 1 that G' and G'' are proportional to ω^2 and ω, respectively, at lower frequency region. Therefore, the rheological parameters in the terminal zone, that is, zero shear viscosity η_0 and steady-state compliance J_e^0, can be determined by the following relations:

$$\eta_0 = \lim_{\omega \to 0} \frac{G''(\omega)}{\omega} \quad (5)$$

$$J_e^0 = \lim_{\omega \to 0} \frac{G'(\omega)}{G''(\omega)^2} \quad (6)$$

Following the equations, η_0 is found to be 4.8 $\times$ 10^3 Pa s for the LL1 and 4.2 $\times$ 10^3 Pa s for the LL2, and J_e^0 is to be 4.2 $\times$ 10^{-5} Pa^{-1} for the LL1 and 1.8 $\times$ 10^{-5} Pa^{-1} for the LL2. It should be noted that the magnitude of η_0 for the LL1 is

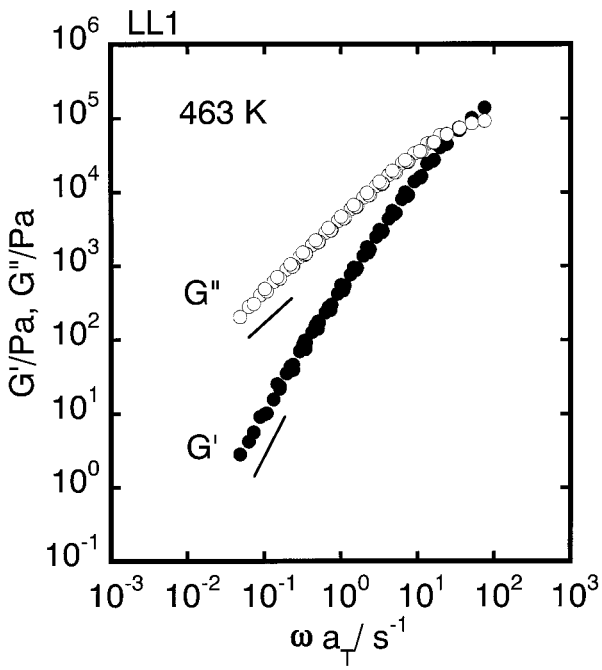

(a)

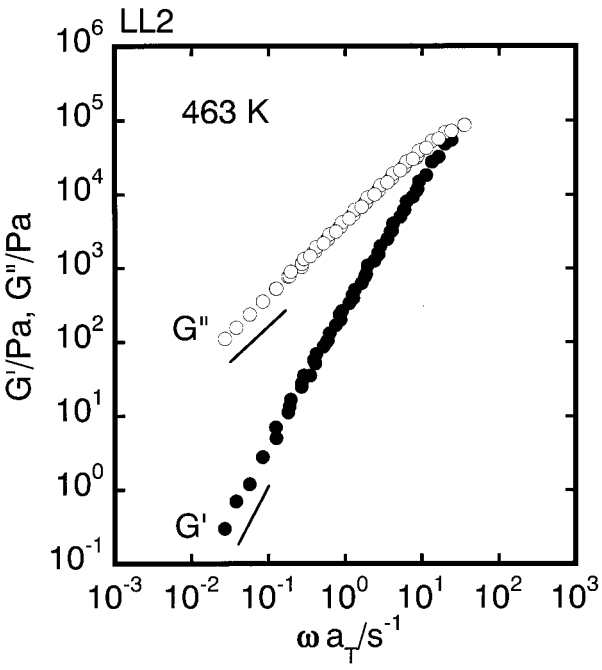

(b)

Figure 1 Master curves of frequency dependence of shear storage modulus G' (●) and loss modulus G'' (○) at 463 K for (a) LL1 and (b) LL2.

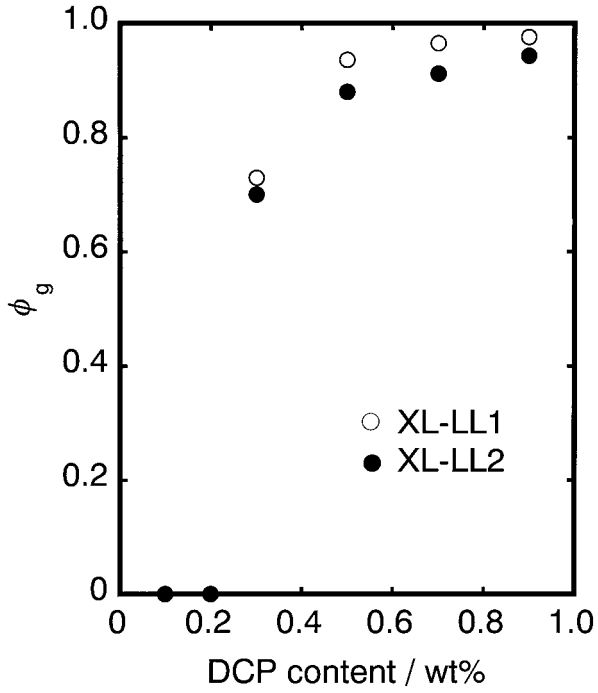

Figure 2 Gel fraction plotted against DCP content for XL-LL1 (○) and XL-LL2 (●).

larger than that for the LL2, although the LL1 has lower M_w than the LL2. Vega et al.[16] have demonstrated that molecular weight dependence of η_0 deviates from the values estimated by the following relation proposed by Raju et al.,[17] as increasing the number of short chain branches.

$$\eta_0 = 3.40 \times 10^{-15} M_w^{3.60} \tag{7}$$

Also in this study, the deviation from the relation is more prominent for the LL1, which has a lot of short chain branches. Moreover, J_e^0 for the LL1 much deviate from the value of high density polyethylene, which is calculated by eq. (8) proposed by Mills[18]:

$$J_e^0 = 2.5 \times 10^{-6} \times \left(\frac{M_z}{M_w}\right)^{3.7} \tag{8}$$

The result indicates that the molecular characteristics, such as plateau modulus and/or critical molecular weight for entanglements, deviate from those of the linear polyethylene as increasing the short chain branches. It has been reported that the plateau modulus decreases with increasing the short chain branches.[19]

Characterization of XL-LL

The gel fraction ϕ_g of the XL-LLs is plotted against the DCP content in Figure 2. The gel fraction is formed beyond 0.3 wt % of the DCP content, whereas both the XL-LL1(0.2) and XL-LL2(0.2) have no gel fraction. Therefore, the critical amount of the DCP for the gelation is estimated to be between 0.2 and 0.3 wt %. Beyond 0.3 wt %, $\phi_g$increases monotonically. Furthermore, ϕ_g of the XL-LL1 is slightly larger than that of the XL-LL2 at the same level of the DCP content.

Figure 3 shows the degree of swelling q of the gel fraction for the XL-LLs. As increasing the DCP content, q decreases rapidly. The magnitude of q of the XL-LL1 is almost the same as those of the XL-LL2. The molecular weight between crosslinking points M_c is calculated by

$$M_c = \frac{1}{\nu^* V} \tag{9}$$

Moreover, the network chain density ν^* is given by q using the theory of Flory and Rehner.[20]

$$\nu^* = -\frac{\ln(1 - q^{-1}) + q^{-1} + \chi q^{-2}}{V(q^{-1/3} - 0.5q^{-1})} \tag{10}$$

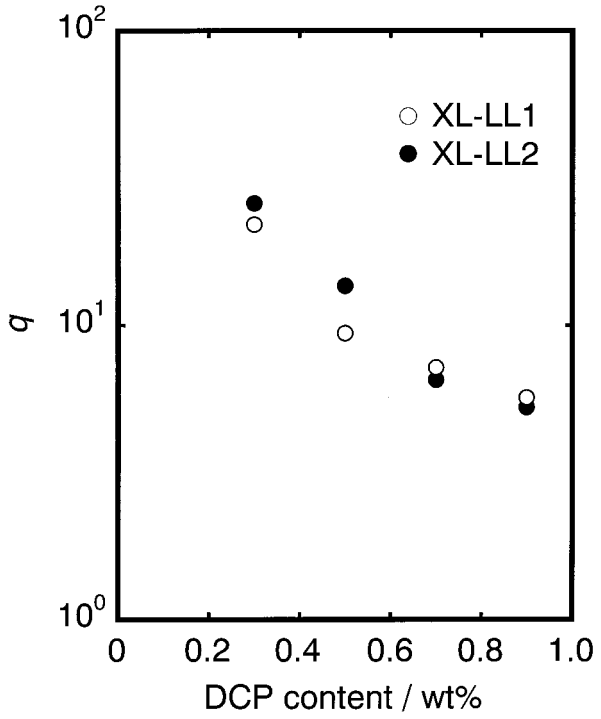

Figure 3 Degree of swelling plotted against DCP content for XL-LL1 (○) and XL-LL2 (●).

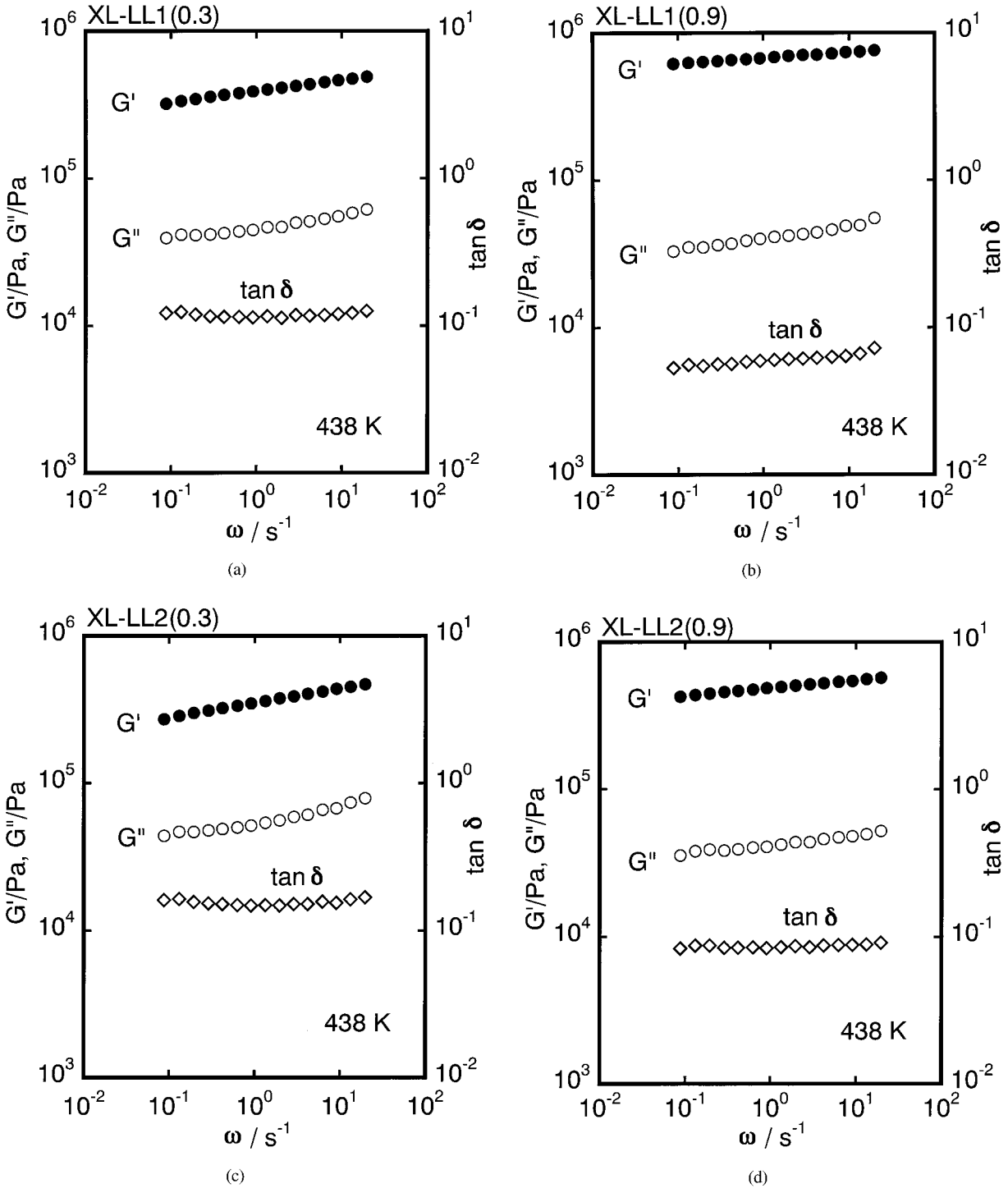

Figure 4 Frequency dependence of storage modulus G' (●), loss modulus G'' (○), and loss tangent tan δ (◇) at 463 K for (a) XL-LL1(0.3), (b) XL-LL1(0.9), (c) XL-LL2(0.3), and (d) XL-LL2(0.9).

where **V** the partial molar volume of the swelling solvent and χ the Flory–Huggins interaction parameter. We use the following values according to the literature[11]: V =136 mL/mol and χ = 0.37.

As a result, the M_c of the XL-LLs is estimated to be 10^4–10^6, which is much larger than the average molecular weight between the entanglement coupling by points of PE.[21–23]

Figure 4 exemplifies the frequency dependence of oscillatory shear moduli for some of the XL-LLs. As seen in the figures, both G' and G'' increase with the DCP content. Furthermore, tanδ is almost independent of the frequency. Valles et al. have studied the viscoelastic properties for the radiation-crosslinked polyethylene,[24] in which the polyethylene with narrow molecular weight distribution (M_w/M_n = 1.14) is employed. They have demonstrated that the crosslinked polyethylene shows the scaling behavior in a very broad vicinity of the gel point. Consequently, tanδ keeps a constant value in the wide range of frequency. Their result is the similar to the present one. Furthermore, the magnitude of G' is much larger than that of G'' even for the XL-LLs containing 0.3 wt % of DCP, which are just beyond the critical gel, suggesting that the XL-LL containing the high level of DCP behaves as like a rubber. Figure 5 shows the storage modulus G' for the XL-LLs. The XL-LL1 exhibits higher value than the XL-LL2 at the same level of the DCP content. Moreover, the XL-LL1(0.9) shows higher G' than the XL-LL2(0.5), although they have almost the same gel fraction. The modulus seems to be determined by both gel fraction and density of crosslink point.

Figure 6 shows the stress–strain curves for the XL-LL1 [Fig. 6(a)] and the XL-LL2 [Fig. 6(b)] at 438 K. In the figure, λ represents the extension ratio. Neither necking nor brittle behavior is observed in this strain region for all samples. The stress level for the XL-LL corresponds with the magnitude of storage modulus.

The stress–strain curves are characterized by using the Mooney–Rivlin equation:

$$\sigma = \left(2C1 + \frac{2C2}{\lambda}\right)\left(\lambda - \frac{1}{\lambda^2}\right) \qquad (11)$$

where σ is the nominal stress, λ is the extension ratio, and $C1$ and $C2$ are constants. According to numerous studies,[25–27] it is considered that both trapped entanglements and crosslinks contribute to $C1$ and $C2$ is associated with trapped entanglements only. In Figure 7, $\sigma/2(\lambda - \lambda^{-2})$ is plotted as a function of λ^{-1} for the XL-LLs. The stress–strain curves are found to be expressed by eq. (11) in the experimental strain region. Therefore, both $C1$ and $C2$ terms can be calculated. Figure 8 shows the relation between DCP content and both $C1$ and $C2$ terms. As seen in the figure, $C2$ terms are larger than $C1$ terms, which indicates trapped entanglements play an important role for the

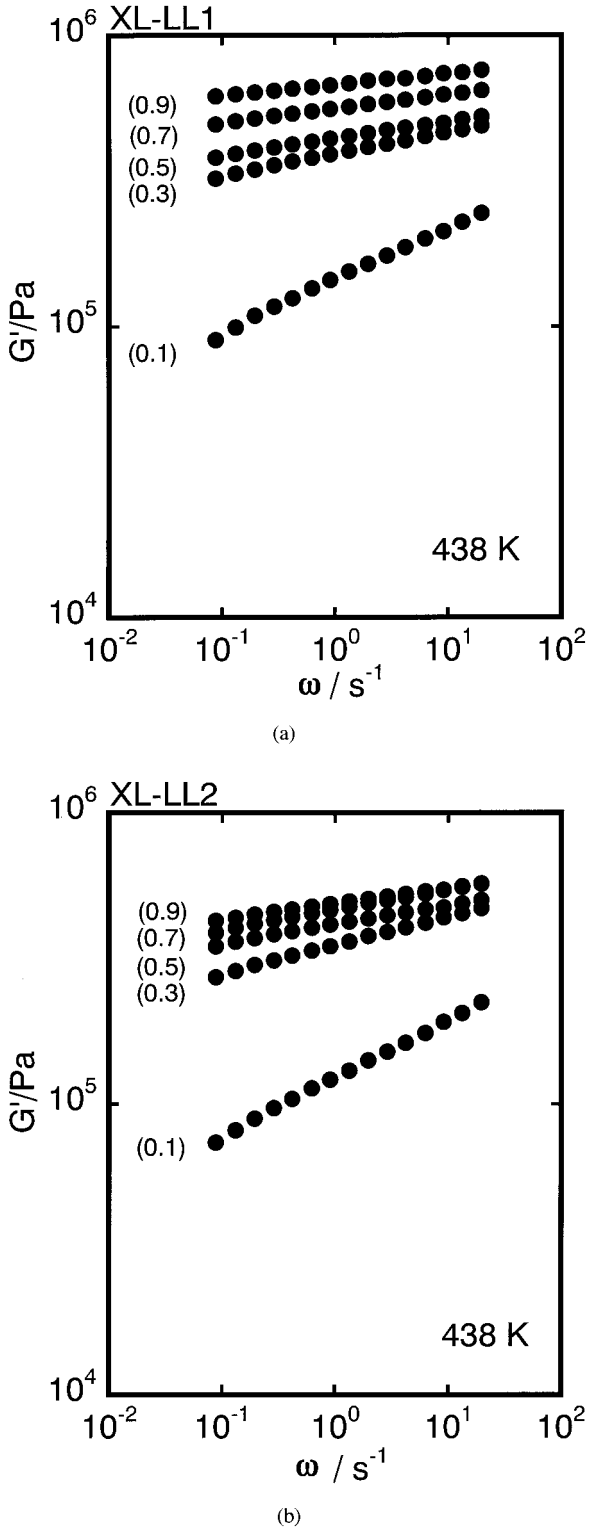

Figure 5 Frequency dependence of storage modulus G' at 438 K for (a) XL-LL1 and (b) XL-LL2. The numerals in the figure denote the DCP content (wt %).

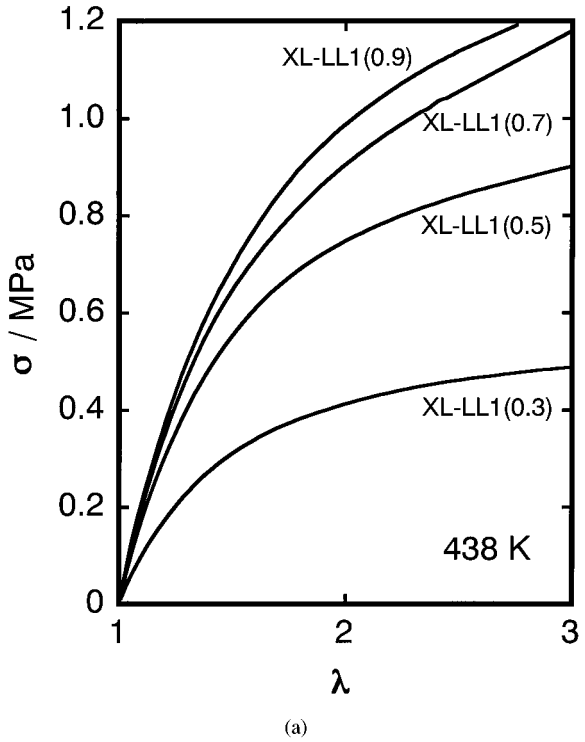

(a)

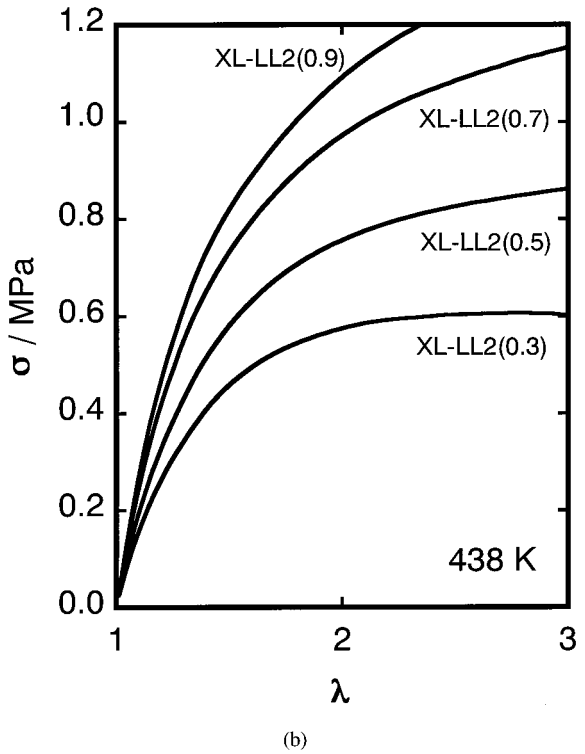

(b)

Figure 6 Stress–strain curves of (a) XL-LL1 and (b) XL-LL2 with different DCP contents at 438 K. The numerals in the figure denote the DCP content (wt %). In the figure, λ represents the extension ratio.

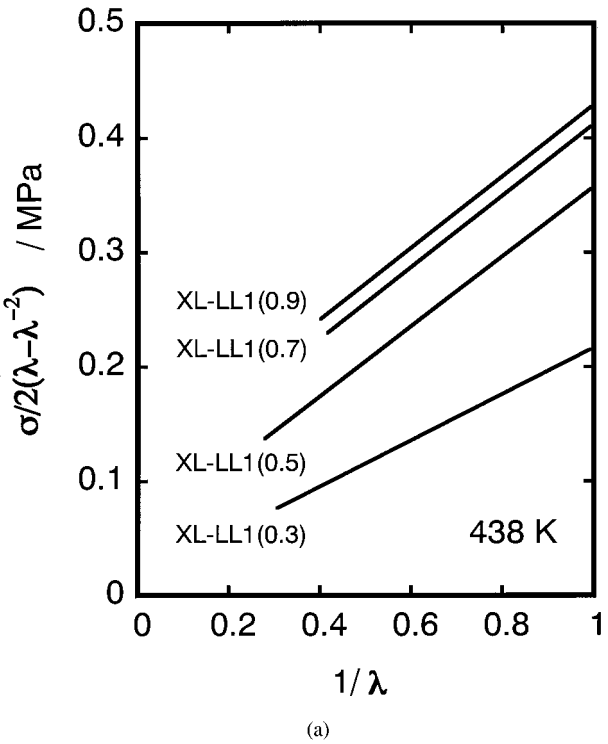

(a)

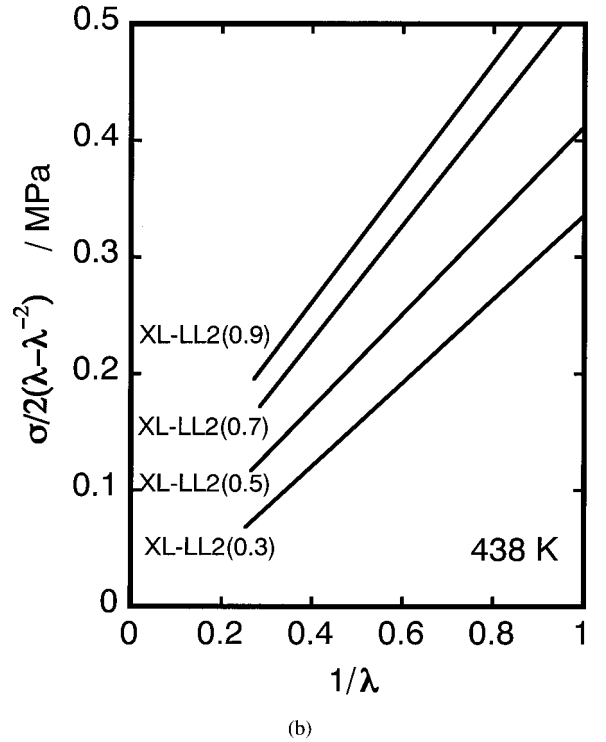

(b)

Figure 7 Mooney–Rivlin plots of (a) XL-LL1 and (b) XL-LL2.

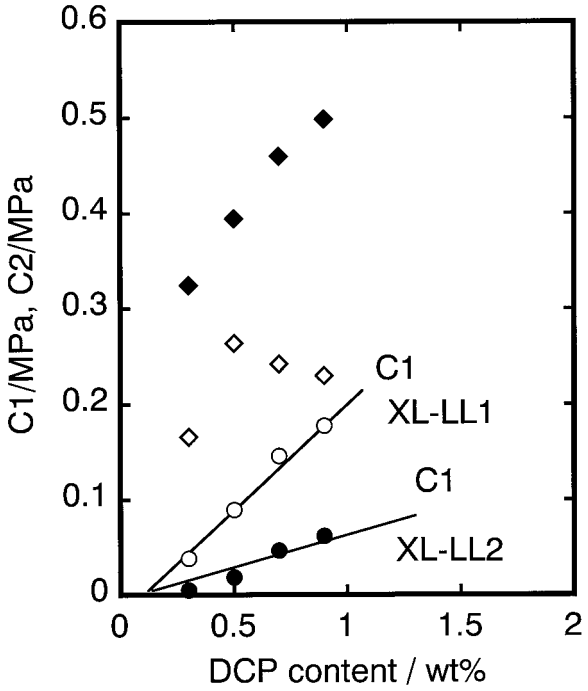

Figure 8 Relation between DCP content and $C1$ (circles) and $C2$ (diamonds) terms for XL-LL1 and XL-LL2. Open symbols represent constants for XL-LL1 and closed ones for XL-LL2.

stress–strain behavior. Moreover, the $C1$ term increases linearly with the DCP content. From the intersection of the x-axis, the critical amount of the DCP content for the gelation is estimated to be between 0.2 and 0.3 wt % for both the XL-LL1 and the XL-LL2, which is in good agreement with the gel fraction measurement as shown in Figure 2. Moreover, the order of the sum of $C1$ and $C2$ terms, which represents the elastic modulus at the limit of the small strain, coincides with that of the oscillatory storage modulus.

Figure 9 shows the peak temperature of crystallization T_c for the XL-LLs. It is obvious that T_c of the XL-LL2 is much higher than that of the XL-LL1 irrespective of the DCP content. Furthermore, it is also found that the depression of T_c due to crosslinking is not so large for both XL-LLs.

Structure of the Foams

Mechanical properties of XL-PE foams, which is characterized, in general, as closed-cell structure, are much affected by the expansion ratio. According to Hosoda et al.,[28] expansion ratio E_R of XL-LD foams is determined by the gel fraction as far as the amount of a blowing agent is constant. Also in this study, E_R decreases with increasing the gel fraction ϕ_g as shown in Figure 10. Moreover, it is impossible to produce the foam, in which ϕ_g is below 0.7. The gel fraction, however, dose not govern the expansion ratio. Relation between DCP content and E_R depends on the species of the LL. This is plausible because the rheological properties are not determined only by the gel fraction. Nevertheless, even considering the rheological properties, we cannot predict the expansion ratio exactly. For example, the XL-LL1(0.5) foam exhibits slightly larger E_R than the XL-LL2(0.7) foam, although the XL-LL1(0.5) shows lower G'. Moreover, E_R of the XL-LL2(0.9) foam is as same as that of the XL-LL1(0.7) foam, although the XL-LL2(0.9) shows higher G'. The difference in the crystallization temperature will be responsible for the phenomena. After expansion, the gas in the cell, which is produced by the decomposition of the blowing agent, lessens its volume owing to the cooling. Therefore, the XL-LL foams show the elastic recovery, that is, shrinkage, prior to the crystallization. As a result, the crystallization temperature of the foams has a significant influence on the shrinkage, hence expansion ratio. The XL-LL foam with high T_c cannot exhibit the large magnitude of elastic recovery, because

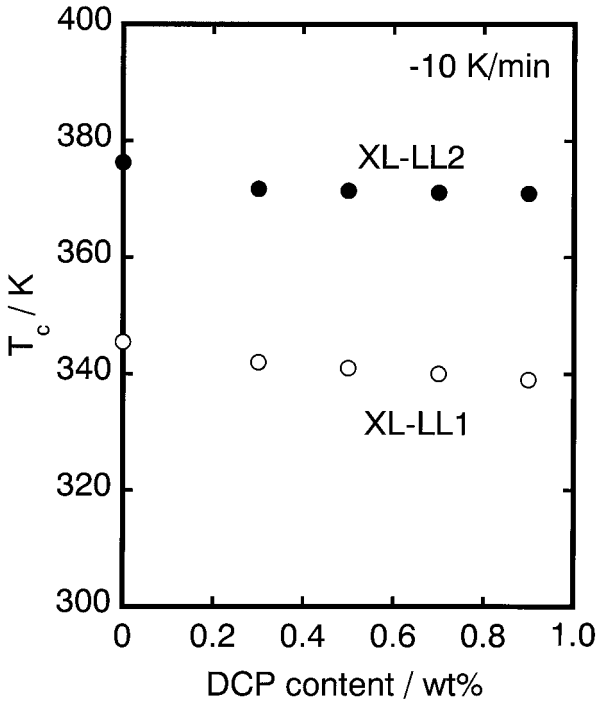

Figure 9 Relation between DCP content and crystallization temperature T_c for XL-LL1 (○) and XL-LL2 (●).

the immediate crystallization prevents the molecular motion to a great degree. Figure 11 shows the time variation of the dimension in length of the foams after taking out from the mold. The XL-LL1(0.5) foam shows a marked shrinkage ascribed to the elastic recovery. On the other hand, the XL-LL2(0.7) foam shows only small shrinkage owing to the crystallization. Accordingly, the XL-LL1(0.5) foam exhibits larger E_R, although it shows lower G' than the XL-LL2(0.7). Thus, the thermal properties, which is responsible for the shrinkage, also affect the expansion ratio as well as the rheological properties.

CONCLUSIONS

The foam processing properties of peroxide-crosslinked linear low-density polyethylenes have been investigated. In this study, two types of the LL produced by a metallocene catalyst, which has different number of short chain branches are used. It was found that both gel fraction and crosslink density determines the rheological properties, such as oscillatory shear modulus and stress–strain curves, of the XL-LL. The expansion ratio of the XL-LL foam is decided by the following two factors. The one is the elastic modulus of the crosslinked materials. As increasing the elastic modulus, the expansion ratio of the foams decreases. The other is the crystallization temperature T_c. The sample with lower T_c exhibits the marked shrinkage after ejecting from the mold, which is the elastic recovery due to the volume reduction of the gas. The degree of shrinkage decreases with increasing the T_c, because immediate crystallization prevents the shrinkage.

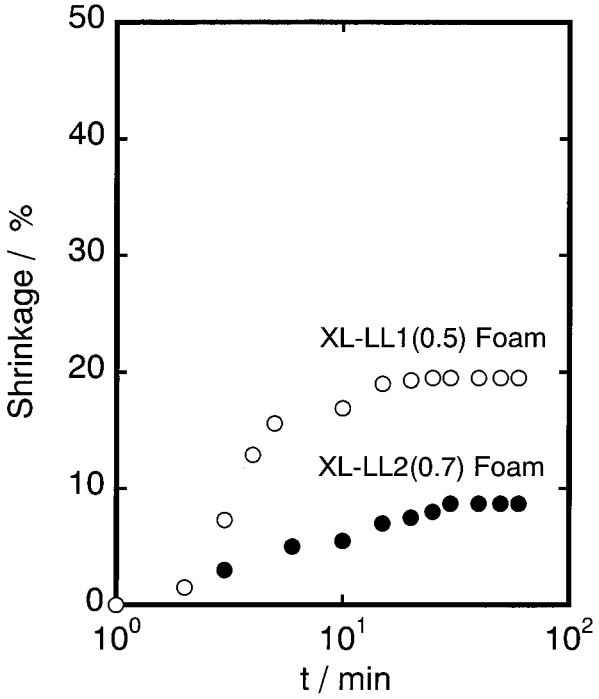

Figure 11 Time variation of dimension in length after ejecting from the mold for XL-LL1(0.5) foam (○) and XL-LL2(0.7) foam (●).

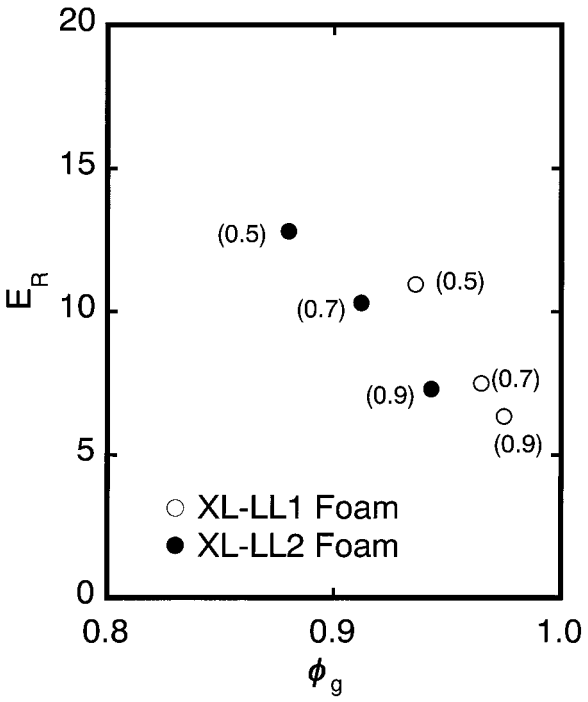

Figure 10 Gel fraction ϕ_g dependence of expansion ratio E_R for XL-LL1 foam (○) and XL-LL2 foam (●). The numerals in the figure denote the DCP content (wt %).

REFERENCES

1. Lasman, H. R. SPE J 1962, 1, 180.
2. Benning, C. J. Cell Plast 1967, 3, 62.
3. Benning, C. J. Cell Plast 1967, 3, 125.
4. Cram, D. J. Robber Plast Age 1968, 49, 11.
5. Bensason, S.; Minick, J.; Moet, A.; Chum, S. P.; Hiltner, A.; Bear, E. J Polym Sci Polym Phys Ed 1996, 34, 1301.
6. Minick, J.; Moet, A., Bear, E.; Chum, S. P. J Appl Polym Sci 1996, 58, 1371.
7. Bensason, S.; Stepanov, E. V.; Chum, S. P.; Hiltner, A.; Bear, E. Macromolecules 1997, 30, 2436.
8. Matthews, R. G.; Ward, I. M.; Capaccio, G. J Polym Sci Polym Phys Ed 1999, 37, 51.

9. Yamaguchi, M.; Abe, S. J Appl Polym Sci 1999, 74, 3153.
10. Yamaguchi, M.; Abe, S. J Appl Polym Sci 1999, 74, 3160.
11. de Boer, A. P.; Penning, A. J. J Polym Sci Polym Phys Ed 1976, 14, 187.
12. Alamo, R. G.; Domszy, R.; Mandelkern, L. J Phys Chem 1984, 51, 887.
13. Alamo, R. G.; Viers, B. D.; Manddelkern, L. Macromolecules 1993, 26, 5740.
14. Alamo, R. G.; Mandelkern, L. Macromolecules 1989, 22, 1273.
15. Vega, J. F.; Santamaria, A.; Munoz-Escalona, A.; LaFuente, P. Macrolecules 1998, 31, 3639.
16. Vega, J. F.; Munoz-Escalona, A.; Santamaria, A.; Munoz, M.; Lufuente, P. Macromol Chem Phys 1999, 200, 2257.
17. Raju, V. R.; Smith, G. G.; Marin, G.; Knos, J. R.; Graessley, W. W. J Polym Sci Polym Phys Ed 1979, 17, 1183.
18. Mills, N. J. Nature 1968, 219, 1249.
19. Yamaguchi, M.; Suzuki, K.; Miyata, H. J Polym Sci Polym Phys Ed 1999, 37, 701.
20. Flory, P. J.; Rehner, Jr. J Chem Phys 1943, 11, 521.
21. Raju, V. R.; Rachapudy, H.; Graessley, W. W. J Polym Sci Polym Phys Ed 1979, 17, 1223.
22. Carella, J. M.; Graessley, W. W.; Fetters, L. Macromolecules 1984, 17, 2775.
23. Porter, R. S.; Johnson, J. F. Chem Rev 1996, 66, 1.
24. Valles, E. M.; Carella, J. M.; Winter, H. H.; Baumgaertel, M. Rheol Acta 1990, 29, 535.
25. Ferry, J. D. Viscoelastic Properties of Polymers, 3rd ed.; John Wiley & Sons: New York, 1980.
26. Flory, P. J.; Erman, B. Macromolecules 1982, 15, 800.
27. Edward, S. F.; Viglis, T. Polymer 1986, 27, 483.
28. Hosoda, K.; Shiina, N.; Ueno, H. Koubunshi Ronbunshu 1977, 34, 585.